

Universal Codes for the Gaussian MAC via Spatial Coupling

Arvind Yedla, Phong S. Nguyen, Henry D. Pfister, and Krishna R. Narayanan
Department of Electrical and Computer Engineering, Texas A&M University
Email: {yarvind,psn,hpfister,krn}@tamu.edu

Abstract— We consider transmission of two independent and separately encoded sources over a two-user binary-input Gaussian multiple-access channel. The channel gains are assumed to be unknown at the transmitter and the goal is to design an encoder-decoder pair that achieves reliable communication for all channel gains where this is theoretically possible. We call such a system *universal* with respect to the channel gains.

Kudekar et al. recently showed that terminated low-density parity-check convolutional codes (a.k.a. spatially-coupled low-density parity-check ensembles) have belief-propagation thresholds that approach their maximum a-posteriori thresholds. This was proven for binary erasure channels and shown empirically for binary memoryless symmetric channels. It was conjectured that the principle of spatial coupling is very general and the phenomenon of threshold saturation applies to a very broad class of graphical models. In this work, we derive an area theorem for the joint decoder and empirically show that threshold saturation occurs for this problem. As a result, we demonstrate near-universal performance for this problem using the proposed spatially-coupled coding system.

Index Terms— Gaussian MAC, LDPC codes, spatial coupling, EXIT functions, density evolution, joint decoding, protograph, area theorem.

I. INTRODUCTION

The phenomenon of threshold saturation was introduced by Kudekar et al. [1] to explain the impressive performance of convolutional LDPC ensembles [2], [3]. They observed that the belief-propagation (BP) threshold of a spatially-coupled ensemble is very close to the maximum-a-posteriori (MAP) threshold of its underlying ensemble; a similar statement was formulated independently, as a conjecture in [4]. This phenomenon has been termed “threshold saturation via spatial coupling”. Kudekar et al. prove in [1] that threshold saturation occurs for the binary erasure channel (BEC) and a particular convolutional LDPC ensemble and conjecture that the phenomenon of threshold saturation is very general. Empirical evidence of this phenomenon has also been shown for additive white Gaussian noise (AWGN) channels in [5] and for a class of channels with memory (the dicode erasure channel) in [6], using EXIT-like curves. It is known that the MAP threshold of regular LDPC codes approaches the Shannon limit with increasing left degree, while keeping

the rate fixed (though such codes have a vanishing BP threshold) [1]. So, spatial coupling appears to provide us with a new paradigm to construct capacity approaching codes for BMS channels.

Spatial-coupling is now being applied to more general scenarios. The noisy Slepian-Wolf problem was considered in [7] and the authors showed that the phenomenon of threshold saturation extends to multi-terminal problems. Threshold saturation was shown for the binary-adder channel with erasures in [8] by considering EXIT-like curves. Spatially-coupled codes have also been shown to achieve the entire rate-equivocation region for the BEC wiretap channel [9]. The effect of coupling has also been observed for K -satisfiability, graph coloring and the Curie-Weiss model of statistical physics in [10], and for compressive sensing in [11] by using spatially-coupled measurement matrices.

The notion of universality with respect to channel parameters was considered in [12, p. 398] and [13] in the context of compound channels. Yedla et al. focused on the notion of universality with respect to channel parameters for multi-terminal problems in [14] and showed that spatially-coupled codes are near-universal for the noisy Slepian-Wolf problem in [7]. Preliminary results in [7] show that spatial coupling increases the threshold for transmission over the binary-input Gaussian multiple-access channel (MAC) as well.

In this paper, we consider the performance of spatially-coupled codes for transmission over the 2-user binary-input Gaussian MAC and investigate the phenomenon of threshold saturation for this problem. The Gaussian MAC has been extensively studied in the literature and is defined by

$$Y = h^{[1]}X^{[1]} + h^{[2]}X^{[2]} + N. \quad (1)$$

The system model is shown in Fig. 1. The channel inputs $X^{[1]}, X^{[2]} \in \{\pm 1\}$ and the variation in channel gains $h^{[1]}, h^{[2]} \in [0, \infty)$ can be explained either by fading or by different power constraints for the two users. The noise N is a zero-mean Gaussian random variable, with fixed variance of 1. The capacity region is defined as the set of all achievable rate tuples $(R^{[1]}, R^{[2]})$, given by the equations

$$\begin{aligned} R^{[1]} &\leq I(X^{[1]}; Y|X^{[2]}) \\ R^{[2]} &\leq I(X^{[2]}; Y|X^{[1]}) \\ R^{[1]} + R^{[2]} &\leq I(X^{[1]}, X^{[2]}; Y). \end{aligned} \quad (2)$$

This material is based upon work supported, in part, by the National Science Foundation (NSF) under Grant No. 0747470, by the Texas Norman Hackerman Advanced Research Program under Grant No. 000512-0168-2007, and by Qatar National Research Foundation. Any opinions, findings, conclusions, and recommendations expressed in this material are those of the authors and do not necessarily reflect the views of these sponsors.

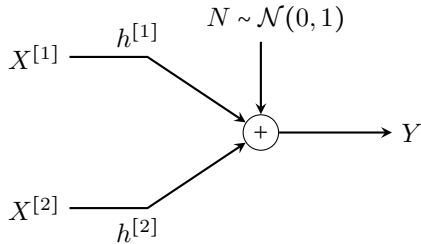


Fig. 1. The Gaussian MAC

The corner points of the capacity region are known to be achievable by combining successive cancellation at the decoder with single-user codes [15]. This method can also be leveraged to achieve any point on the dominant face by time sharing or rate splitting [16]. The problem of designing good LDPC degree distributions was studied in [17] using density evolution (DE), where the authors design good LDPC codes for a few points in the achievable region (in terms of rate). Another approach was shown in [18] for the case when both users have the same transmit power, using EXIT charts.

These optimization procedures exploit knowledge of the channel gains to design good codes. However, in practical scenarios the channel gains cannot be known non-causally at the transmitter (for example, a fading channel). So, it is desirable to fix the rate pair for transmission and view the capacity region in terms of the achievable channel gains for that rate pair. In other words, the capacity region is the set of all channel gains $(h^{[1]}, h^{[2]})$ that are achievable, i.e., satisfy (2). We call this region as the MAC achievable channel-parameter region (MAC-ACPR), to illustrate that the capacity region is defined in terms of achievable channel parameters. The achievable channel parameter regions (ACPRs) were introduced in [19] as reliable channel regions, in the context of communication over parallel channels. As the channel gains are not known at the transmitter, it is desirable to use codes which can simultaneously achieve the entire MAC-ACPR (in order to minimize the outage probability for fading channels).

Coding schemes which can achieve the entire rate region are said to be *universal*. However, LDPC codes optimized for a fixed 2-user binary-input Gaussian MAC need not perform well for different channel parameters. Fig. 2 shows the belief propagation achievable channel parameter region (BP-ACPR), computed via density evolution (DE), of an LDPC ensemble optimized for the equal power case [20, p. 311]. Even though the performance is close to capacity for the equal power case, the performance is far from optimal for asymmetric channel gains. So we need to consider additional constraints when optimizing irregular LDPC codes to achieve universality. Spatially-coupled codes have been shown (via numerical computation of the BP-ACPR) to provide near-universal performance for the noisy Slepian-Wolf problem [7]. In this paper, we consider spatially-coupled codes as a potential candidate to achieve universality for this problem.

To simplify notation, we assume that both users employ different codes of rate R , from the same ensemble. We use spatially-coupled codes for this problem and provide numer-

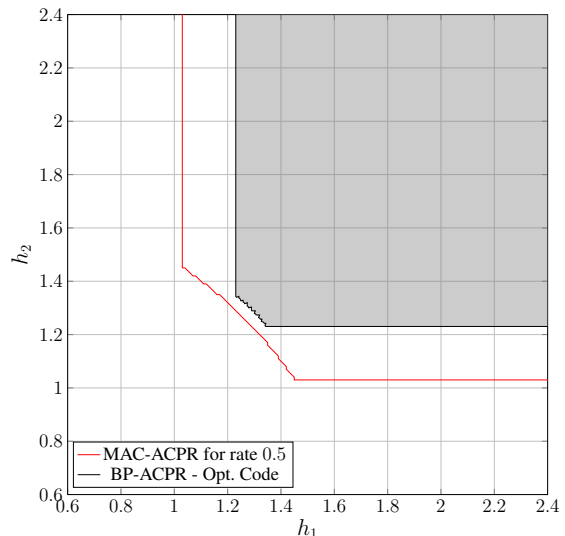


Fig. 2. BP-ACPR for an LDPC code optimized for the equal rate, equal power case and the MAC-ACPR for rate 1/2. The degree profiles can be found in [20, p. 311].

ical evidence for the phenomenon of threshold saturation. Analogous to the MAP threshold for point-to-point communication, one can define a MAP boundary for multi-terminal scenarios. An appropriate GEXIT kernel is also defined to construct GEXIT curves for this problem. These GEXIT curves satisfy the area theorem by definition and provide an outer bound to the MAP boundary. The threshold saturation phenomenon is observed to occur towards the MAP boundary i.e., the BP-ACPR boundary saturates towards the MAP boundary. This provides numerical evidence that supports the conjecture that the outer bound on the MAP boundary, computed via the area theorem, is tight. The MAP boundary for the $(4, 8)$ regular LDPC ensemble is observed to be close to the boundary of the MAC-ACPR, thereby showing that spatially-coupled codes provide near-universal performance for this problem. To the knowledge of the authors, this is currently the only practical coding scheme that achieves near-universal performance for this problem.

The paper is organized as follows: In Section II, we describe DE for the joint iterative decoder and the GEXIT curves used to identify the upper bounds on the MAP threshold are discussed in Section II-E. We briefly discuss spatial coupling in Section III and density evolution for spatially-coupled codes in Section III-B. The results are presented in Section IV.

II. DENSITY EVOLUTION AND GEXIT CURVES

In this section, we briefly cover some notation and background for LDPC codes, the 2-user binary-input Gaussian MAC and density evolution. We will then discuss GEXIT curves for the joint iterative decoder and use them to compute an outer bound on the MAP boundary.

A. Background

An LDPC ensemble can be characterized by its degree profiles. Based on standard notation [20], we let $\lambda(x) =$

$\sum_i \lambda_i x^{i-1}$ be the degree distribution (from an edge perspective) corresponding to the variable nodes and $\rho(x) = \sum_i \rho_i x^{i-1}$ be the degree distribution (from an edge perspective) of the parity-check nodes in the decoding graph. The coefficient λ_i (resp. ρ_i) gives the fraction of edges that connect to variable nodes (resp. parity-check nodes) of degree i . Likewise, L_i is the fraction of variable nodes with degree i . The design rate of an LDPC ensemble is given by

$$r(\lambda, \rho) = 1 - \frac{\int_0^1 \rho(x) dx}{\int_0^1 \lambda(x) dx}.$$

B. The joint iterative decoder

Let $\mathbf{X}^{[1]}, \mathbf{X}^{[2]} \in \{\pm 1\}^n$ denote the input of users 1 and 2 respectively and \mathbf{Y} denote the received vector. We consider the case when both users employ LDPC codes for transmission. To simplify notation, we assume that both the users encode the data using LDPC codes from the standard irregular ensemble LDPC(n, λ, ρ) and that the transmission is bit-aligned. The factor graph of the joint decoder (see Fig. 3) consists of two single user Tanner graphs, whose variable nodes are connected through a function node [20, p. 308]. The variable nodes that are connected via the function node are chosen at random¹. We also assume that the joint decoder iterates by performing one round of decoding for user one, followed by one round of decoding for user two. Let $X_i = (X_i^{[1]}, X_i^{[2]})$ and $\mathbf{X} = (\mathbf{X}^{[1]}, \mathbf{X}^{[2]})$. Without loss of generality, we can label the elements of $\{\pm 1\}^2$ by integers $\mathcal{X} \triangleq \{0, 1, 2, 3\}$ using the map $\pi : \mathcal{X} \rightarrow \{\pm 1\}^2$, defined by $0 \mapsto (+1, +1), 1 \mapsto (+1, -1), 2 \mapsto (-1, +1)$ and $3 \mapsto (-1, -1)$. Let $\pi_1, \pi_2 : \mathcal{X} \rightarrow \{\pm 1\}$ be the projections onto the first and second coordinate respectively. Then, the canonical representation of the channel output is given by

$$\begin{aligned} \nu_{x_i}(y_i) &= p_{Y|X^{[1]}, X^{[2]}}(y_i | \pi_1(x_i), \pi_2(x_i)) \\ &= \frac{1}{\sqrt{2\pi\sigma^2}} \exp\left[-\frac{(y_i - h^{[1]}\pi_1(x_i) - h^{[2]}\pi_2(x_i))^2}{2\sigma^2}\right]. \end{aligned}$$

Let $m_{i,v \rightarrow f}^{[j]}$ and $m_{i,f \rightarrow v}^{[j]}$ denote the ‘‘variable node to function node’’ and ‘‘function node to variable node’’ messages², respectively, for variable node i of the j th user. Here $j \in \{1, 2\}$ and $i \in \{1, 2, \dots, n\}$. The message passing rules at the function node are given by

$$m_{i,f \rightarrow v}^{[1]} = \log \frac{\nu_0(y_i) e^{m_{i,v \rightarrow f}^{[2]} + \nu_1(y_i)}}{\nu_2(y_i) e^{m_{i,v \rightarrow f}^{[2]} + \nu_3(y_i)}}, \quad (3)$$

$$m_{i,f \rightarrow v}^{[2]} = \log \frac{\nu_0(y_i) e^{m_{i,v \rightarrow f}^{[1]} + \nu_2(y_i)}}{\nu_1(y_i) e^{m_{i,v \rightarrow f}^{[1]} + \nu_3(y_i)}}. \quad (4)$$

Note that this function node operation is not symmetric with respect to the users in general. The operations are the same only for the case of symmetric fading coefficients i.e., when $h^{[1]} = h^{[2]}$.

¹Other matching rules result in a different performance in general.

²Here, the messages are in the log-likelihood domain.

C. Density evolution

Density evolution is employed to analyze the asymptotic performance of the ensemble LDPC(n, λ, ρ). The lack of symmetry means that one cannot use the all-zero codeword assumption for this problem. Instead, one may assume that both users transmit codewords of type one-half, which occurs with high probability (a more thorough discussion can be found in [20, p. 296]). In this case, $p_X(x) = 1/4, \forall x \in \mathcal{X}$. We use the notation $\mathbf{a}_{\text{BAWGNMA}} \triangleq \mathbf{a}_{\text{BAWGNMA}(h^{[1]}, h^{[2]})}$ to denote the density of the received random variable Y . Let $f_{1 \rightarrow 2}(\cdot, \mathbf{a}_{\text{BAWGNMA}})$ (respectively $f_{2 \rightarrow 1}(\cdot, \mathbf{a}_{\text{BAWGNMA}})$) be the density transformation operator corresponding to a message from user 1 to user 2 (user 2 to user 1) via the function node. More precisely,

$$\begin{aligned} f_{1 \rightarrow 2}(\mathbf{a}, \mathbf{a}_{\text{BAWGNMA}}) &\triangleq \sum_{x \in \mathcal{X}} p(x) f_{12}(\mathbf{a}(\pi_1(x)u), \nu_x(u)) \\ f_{2 \rightarrow 1}(\mathbf{b}, \mathbf{a}_{\text{BAWGNMA}}) &\triangleq \sum_{x \in \mathcal{X}} p(x) f_{21}(\mathbf{b}(\pi_2(x)u), \nu_x(u)), \end{aligned}$$

where $f_{12}(\cdot, \cdot)$ and $f_{21}(\cdot, \cdot)$ are density transformation operators corresponding to (3) and (4). Here, $\mathbf{a}(u)$ (respectively $\mathbf{b}(u)$) is the density of the messages $m_{i,v \rightarrow f}^{[1]}$ ($m_{i,v \rightarrow f}^{[2]}$). These operators can be computed numerically for discretized densities following the procedure outlined in [21]. Let \mathbf{a}_ℓ and \mathbf{b}_ℓ denote the L -density³ of the messages emanating from the variable nodes to the check nodes at iteration ℓ , corresponding to codes 1 and 2. Then, the DE equations for the joint decoder are given by

$$\begin{aligned} \mathbf{a}_{\ell+1} &= f_{2 \rightarrow 1}(L(\rho(\mathbf{b}_\ell)), \mathbf{a}_{\text{BAWGNMA}}) \otimes \lambda(\rho(\mathbf{a}_\ell)) \\ \mathbf{b}_{\ell+1} &= f_{1 \rightarrow 2}(L(\rho(\mathbf{a}_\ell)), \mathbf{a}_{\text{BAWGNMA}}) \otimes \lambda(\rho(\mathbf{b}_\ell)), \end{aligned}$$

where $\lambda(\mathbf{a}) = \sum_i \lambda_i \mathbf{a}^{\otimes(i-1)}$, $L(\mathbf{a}) = \sum_i L_i \mathbf{a}^{\otimes(i-1)}$, and $\rho(\mathbf{a}) = \sum_i \rho_i \mathbf{a}^{\otimes(i-1)}$. Here, $L(\rho(\cdot))$ is the density of the messages from the variable node to the function node. These equations accurately represent the evolution of densities at the decoder due to the symmetry of the variable and check node operations. The fixed points of density evolution are the triples $(\mathbf{a}_{\text{BAWGNMA}}, \mathbf{a}, \mathbf{b})$ which satisfy

$$\begin{aligned} \mathbf{a} &= f_{2 \rightarrow 1}(L(\rho(\mathbf{b})), \mathbf{a}_{\text{BAWGNMA}}) \otimes \lambda(\rho(\mathbf{a})) \\ \mathbf{b} &= f_{1 \rightarrow 2}(L(\rho(\mathbf{a})), \mathbf{a}_{\text{BAWGNMA}}) \otimes \lambda(\rho(\mathbf{b})). \end{aligned} \quad (5)$$

Let $\Delta_{+\infty}$ denote the delta function at $+\infty$ and let $h^{[2]} = A \cdot h^{[1]}$, for some $A \in [0, +\infty]$. The BP threshold is defined by

$$\begin{aligned} h^{[1],\text{BP}}(\lambda, \rho, A) &= \sup\{h^{[1]} : \text{The fixed point equation} \\ &\quad (5) \text{ has a solution } (\mathbf{a}, \mathbf{b}) \neq (\Delta_{+\infty}, \Delta_{+\infty})\}, \\ h^{[2],\text{BP}}(\lambda, \rho, A) &= A h^{[1],\text{BP}}(\lambda, \rho, A). \end{aligned}$$

The set of all points $(h^{[1]'}, A h^{[1]'}) \ni h^{[1]'} \geq h^{[1],\text{BP}}(\lambda, \rho, A)$ is called the BP-ACPR and its boundary is called the DE boundary.

³Since the transmission alphabet is $\{\pm 1\}$, the densities are conditioned assuming the transmission of a +1.

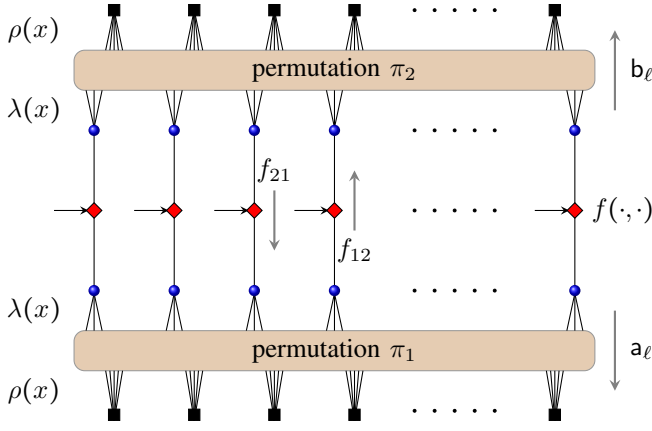


Fig. 3. Tanner graph of the joint decoder. The variable nodes of each code are connected through function nodes, which receives the channel outputs. The joint decoder iterates by passing messages between the component decoders.

D. GEXIT curves

The following approach can be applied to any binary-input MAC characterized by a single parameter, whose density is differentiable and degraded with respect to that parameter. A thorough discussion of channel degradation can be found in [20, p. 204]. The binary-input Gaussian MAC defined by (1) satisfies these conditions for the parameter α , with $h_1 = \alpha$ and $h_2 = A\alpha$, for any fixed $A \in [0, +\infty)$. We note that any differentiable parameterization would suffice for the following discussion.

Now, suppose that the i th bit is transmitted through a channel with parameter α_i and that each α_i is a differentiable function of some parameter α . We omit the dependence of the channel on A throughout this section for clarity of notation. The GEXIT curve is defined by

$$\mathbf{g}(\alpha) \triangleq \frac{1}{n} \sum_{i=1}^n \underbrace{\frac{\partial}{\partial \alpha_i} H(\mathbf{X}|\mathbf{Y}(\alpha))}_{\triangleq \mathbf{g}_i(\alpha_i)} \frac{\partial \alpha_i}{\partial \alpha}.$$

A more convenient expression for the GEXIT curve can be derived following the procedure given in [22] for non-binary codes. Let $\mathbf{y}_{\sim i} = \mathbf{y} \setminus y_i$, $\phi_i(\mathbf{y}_{\sim i}) = \{p_{X_i|Y_{\sim i}}(x|\mathbf{y}_{\sim i}), x \in \mathcal{X}\}$ and $\Phi_i \triangleq \phi_i(\mathbf{Y}_{\sim i})$ be the corresponding random variable. Note that $\phi_i(\cdot)$ is the extrinsic MAP estimator of X_i ⁴.

Lemma 1: Suppose that all bits are transmitted through channel with parameter α . Then, the i th GEXIT function is given by

$$\mathbf{g}_i(\alpha) = \sum_{x \in \mathcal{X}} p(x) \int_{\mathbf{u}} \mathbf{a}_{x,i}(\mathbf{u}) \kappa_x(\mathbf{u}) d\mathbf{u},$$

where $\mathbf{a}_{x,i}(\mathbf{u})$ is the distribution of Φ_i given $X_i = x$ and the

⁴To see this, write

$$p_{\mathbf{Y}_{\sim i}|X_i}(\mathbf{y}_{\sim i}|x_i) = \frac{p_{X_i|Y_{\sim i}}(x_i|\mathbf{y}_{\sim i})}{p_{X_i}(x_i)} p_{\mathbf{Y}_{\sim i}}(\mathbf{y}_{\sim i}) = \frac{\phi_i \cdot e[x_i]}{p_{X_i}(x_i)} p_{\mathbf{Y}_{\sim i}}(\mathbf{y}_{\sim i}),$$

where $e[x_i]$ is the standard basis vector with a 1 in the x_i -th coordinate and use the result in [20, p. 29].

GEXIT kernel is given by

$$\kappa_x(\mathbf{u}) = \int \frac{\partial}{\partial \alpha} p(y|x) \log_2 \frac{\sum_{x'} u[x'] p(y|x')}{u[x] p(y|x)} dy, \quad (6)$$

where $u[j]$ denotes the j th component of \mathbf{u} .

Proof: Suppose that each bit is transmitted through a channel with parameter α_i and consider the term

$$\begin{aligned} H(\mathbf{X}|\mathbf{Y}) &= H(X_i|\mathbf{Y}) + H(\mathbf{X}_{\sim i}|X_i, \mathbf{Y}) \\ &= H(X_i|Y_i, \Phi_i) + H(\mathbf{X}_{\sim i}|X_i, \mathbf{Y}_{\sim i}). \end{aligned}$$

Note that the second term of the decomposition does not depend on the channel at position i . So, we get

$$\mathbf{g}_i(\alpha_i) = \frac{d}{d\alpha_i} H(X_i|Y_i, \Phi_i).$$

We have,

$$\begin{aligned} H(X_i|Y_i, \Phi_i) &= - \iint \sum_x p(x, y, \phi) \log_2 \frac{p(x, y, \phi)}{\sum_{x'} p(x', y, \phi)} dy d\phi \\ &= \sum_x p(x) \int_{\phi} p(\phi|x) \left(\int_y p(y|x) \log_2 \frac{\sum_{x'} p(x'|\phi) p(y|x')}{p(x|\phi) p(y|x)} dy \right) d\phi, \end{aligned}$$

which follows from the fact that

$$p_{X_i, Y_i, \Phi_i}(x, y, \phi) = p(y|x) p(\phi|x) p(x),$$

since $Y_i \rightarrow X_i \rightarrow \Phi_i$. Taking the derivative and noting that $p(x_i|\phi_i) = p(x_i|\mathbf{y}_{\sim i})$, we obtain⁵

$$\begin{aligned} \mathbf{g}_i(\alpha_i) &= \sum_x p(x) \int_{\phi} p(\phi|x) \left(\int_y \frac{\partial}{\partial \alpha} p(y|x) \right. \\ &\quad \left. \log_2 \frac{\sum_{x'} p(x'|\phi) p(y|x')}{p(x|\phi) p(y|x)} dy \right) d\phi \\ &= \sum_x p(x) \int_{\mathbf{u}} \mathbf{a}_x(\mathbf{u}) \kappa_x(\mathbf{u}) d\mathbf{u}, \end{aligned}$$

and the result follows by setting $\alpha_i = \alpha$. \blacksquare

The GEXIT function is hard to compute and hence we use the BP-GEXIT function instead [23]. The BP-GEXIT function is obtained by replacing the MAP extrinsic estimator with the corresponding BP estimator. Let $\Phi_i^{\text{BP}, \ell, n}$ denote the BP extrinsic estimate of X_i after ℓ iterations of the joint decoder. The BP extrinsic estimate is computed using the computation graph of depth ℓ for function node i . Define the BP-GEXIT function at the ℓ th iteration $\mathbf{g}^{\text{BP}, \ell, n}(\alpha)$ in a similar manner to [23] (taking an expectation over all possible computation graphs) and the asymptotic BP-GEXIT function $\mathbf{g}^{\text{BP}}(\alpha) = \lim_{\ell \rightarrow \infty} \lim_{n \rightarrow \infty} \mathbf{g}^{\text{BP}, \ell, n}(\alpha)$. For fixed ℓ , in the limit of $n \rightarrow \infty$, the computation graph becomes tree-like because the computation graphs of the two variable nodes (which themselves become tree-like) connected to the function node do not overlap with high probability. The extrinsic estimate of X_i can then be computed via the

⁵The terms obtained by differentiating with respect to the channel inside the log vanish.

extrinsic estimates of $X_i^{[1]}$ and $X_i^{[2]}$. The asymptotic BP-GEXIT function can be computed through the fixed points of density evolution ($\mathfrak{a}_{\text{BAWGNMA}}(\alpha), \mathfrak{a}, \mathfrak{b}$) which satisfy (5) and is discussed in the following Lemma.

Lemma 2: Consider transmission over the channel $\mathfrak{a}_{\text{BAWGNMA}}(\alpha)$ and let $(\mathfrak{a}_{\text{BAWGNMA}}(\alpha), \mathfrak{a}, \mathfrak{b})$ be a fixed point of DE. Define the BP-GEXIT value of the fixed point by

$$G^{\text{BP}}(\mathfrak{a}_{\text{BAWGNMA}}, \mathfrak{a}, \mathfrak{b}) \triangleq \sum_{x \in \mathcal{X}} p(x) \int F_x[\mathfrak{a}, \mathfrak{b}](u, v) \kappa_x(u, v) du dv.$$

The GEXIT kernel $\kappa_x(\cdot, \cdot)$ is defined as in (6) and the operator $F_x[\cdot, \cdot]$ computes the density of the extrinsic BP estimate Φ^{BP} given $X = x$. The BP-GEXIT curve $\mathfrak{g}^{\text{BP}}(\alpha)$ is given in parametric form by $(\alpha, G(\mathfrak{a}_{\text{BAWGNMA}}(\alpha), \mathfrak{a}, \mathfrak{b}))$.

Proof: Let $\Phi^{\text{BP}} = \mathbf{u}$. Then,

$$\begin{aligned} \mathbf{u} &= \phi(\mathbf{y}_{\sim i}) = \{p(x_i | \mathbf{y}_{\sim i}), x_i \in \mathcal{X}\} \\ &= \{p(\pi_1(x_i) | \mathbf{y}_{\sim i}) \cdot p(\pi_2(x_i) | \mathbf{y}_{\sim i}), x_i \in \mathcal{X}\}. \end{aligned}$$

If we define

$$u \triangleq \log \frac{p(X_i^{[1]} = +1 | \mathbf{y}_{\sim i})}{p(X_i^{[1]} = -1 | \mathbf{y}_{\sim i})}, v \triangleq \log \frac{p(X_i^{[2]} = +1 | \mathbf{y}_{\sim i})}{p(X_i^{[2]} = -1 | \mathbf{y}_{\sim i})},$$

then

$$\begin{aligned} \mathbf{u} &= \left(\frac{e^u}{1 + e^u} \frac{e^v}{1 + e^v}, \frac{e^u}{1 + e^u} \frac{1}{1 + e^v}, \frac{1}{1 + e^u} \frac{e^v}{1 + e^v}, \frac{1}{1 + e^u} \frac{1}{1 + e^v} \right) \\ &\triangleq f(u, v). \end{aligned} \quad (7)$$

Let $\mathfrak{a}(u)$ denote the density of U conditioned on $X_i^{[1]} = +1$ and $\mathfrak{b}(v)$ be the density of V conditioned on $X_i^{[2]} = +1$. Then, $\mathfrak{a}(-u)$ is the density of U conditioned on $X_i^{[1]} = -1$ and $\mathfrak{b}(-v)$ is the density of V conditioned on $X_i^{[2]} = -1$. In the limit $n \rightarrow \infty$ and taking expectation these densities are given by the fixed point $(\mathfrak{a}_{\text{BAWGNMA}}(\alpha), \mathfrak{a}, \mathfrak{b})$. Let $F_x[\mathfrak{a}, \mathfrak{b}](u, v)$ be the density of Φ_i^{BP} conditioned on $(X_i^{[1]} = \pi_1(x), X_i^{[2]} = \pi_2(x))$. Then,

$$F_x[\mathfrak{a}, \mathfrak{b}](u, v) = \mathfrak{a}(\pi_1(x)u) \mathfrak{b}(\pi_2(x)v).$$

For example $F_0[\mathfrak{a}, \mathfrak{b}](u, v) = \mathfrak{a}(u)\mathfrak{b}(v)$, $F_1[\mathfrak{a}, \mathfrak{b}](u, v) = \mathfrak{a}(u)\mathfrak{b}(-v)$ and so on. The result follows by the definition of the GEXIT curve. The kernels $\kappa_x(u, v)$ are defined in the sense of (7). ■

It can be shown that the BP-GEXIT function is an upper bound on the GEXIT function (see the discussion in [20, p. 206]). The BP-GEXIT curve for the LDPC(3, 6) ensemble is shown in Fig. 4, for $A = 1$.

E. The MAP Boundary

Let $h_i^{[1]}(\alpha) = \alpha$ and $h_i^{[2]}(\alpha) = A\alpha$, for all $i = 1, \dots, n$. Consider transmission using codes from the ensemble LDPC(n, λ, ρ). For a fixed A , we define the MAP threshold as

$$\alpha^{\text{MAP}}(A) = \inf \left\{ \alpha : \liminf_{n \rightarrow \infty} \frac{1}{n} \mathbb{E}[H(\mathbf{X} | \mathbf{Y}(\alpha, A))] > 0 \right\},$$

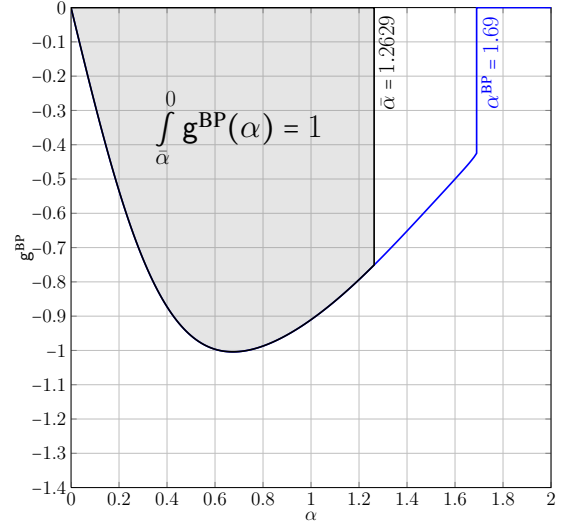


Fig. 4. BP-GEXIT curve and an upper bound on the MAP threshold (computed using the area theorem), for $A = 1$, of the (3, 6) regular LDPC ensemble. GEXIT curves in literature are typically parameterized by the channel entropy and the channels get *worse* as the entropy increases. However, the channel gains are a natural parameterization for this problem and the channel gets *better* by increasing the channel gains. So the GEXIT values are negative for this parameterization.

where the expectation is taken over all codes in the ensemble. The set of all points $(\alpha', A) \ni \alpha' \geq \alpha^{\text{MAP}}(A)$ form the MAP-ACPR and its boundary is called the MAP boundary. By definition of the GEXIT function, this gives

$$\begin{aligned} \int_{+\infty}^0 \mathfrak{g}(\alpha) d\alpha &= \frac{1}{n} \int_{+\infty}^0 \frac{dH(\mathbf{X} | \mathbf{Y}(\alpha))}{d\alpha} d\alpha \\ &= \frac{1}{n} H(\mathbf{X} | \mathbf{Y}(0)) \\ &= \frac{2k}{n}. \end{aligned}$$

The above equation gives us a procedure to compute the MAP threshold, using the GEXIT curve. Let $\bar{\alpha}$ denote the largest positive number such that

$$\int_{\bar{\alpha}}^0 \mathfrak{g}^{\text{BP}}(\alpha) d\alpha = 2r(\lambda, \rho),$$

where $r(\lambda, \rho)$ is the design rate of the ensemble LDPC(λ, ρ). Then the MAP threshold $\alpha^{\text{MAP}} \leq \bar{\alpha}$. The upper bound on the MAP threshold is shown in Fig. 4 for the (3, 6) LDPC ensemble, for $A = 1$. Using this procedure, we can compute an outer bound to the MAP boundary by considering different values of A .

III. SPATIAL COUPLING

Spatial coupling is best described by the (l, r, L) ensemble through a protograph [1], [24]. The protograph structure at the joint decoder is shown in Fig. 5 for a LDPC(3, 6) base code. The protograph is generated as follows: Consider the protograph of a (3, 6) regular LDPC code. It has two variable nodes of degree 3 and one check node of degree 6. Connect both the variable nodes to the variable nodes of another protograph via function nodes. The resulting protograph represents the joint decoder when both users are using (3, 6)

regular LDPC codes for transmission over the 2-user binary-input Gaussian MAC. Place $2L + 1$ protographs at positions $-L, \dots, L$. Each of the 3 edges of a variable node at position i is connected to exactly one check node at position $i-1, i, i+1$, for each user.

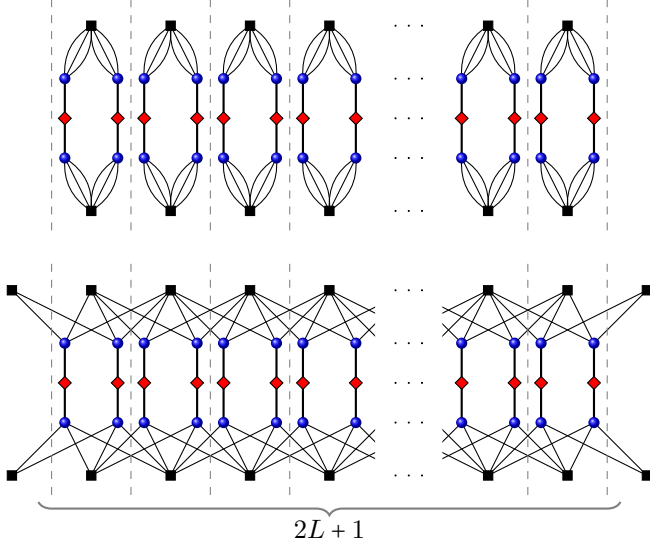


Fig. 5. Protograph of the joint decoder. Shown above are $2L + 1$ copies of the protograph of the joint decoder for a $(3,6)$ regular LDPC code. The bottom graph shows the protograph of the joint decoder for the corresponding spatially coupled code.

Although this ensemble is very instructive in understanding the universality of spatially-coupled codes, the EBP curves for this ensemble exhibit wiggles around the MAP threshold (similar to the single user channels as discussed in [1]). The magnitude of these wiggles appears to remain constant with increasing L and their presence implies that the BP threshold is smaller than the MAP threshold of the underlying ensemble. Therefore, the $(3,6,L)$ ensemble does not exhibit the threshold saturation phenomenon exactly. To overcome this, we use the (l,r,L,w) ensemble introduced in [1] for the remainder of this work.

A. The (l,r,L,w) ensemble

The (l,r,L,w) spatially-coupled ensemble can be described as follows: Place M variable nodes at each position in $[-L,L]$. The check nodes are placed at positions $[-L, L+w-1]$, with $\frac{l}{r}M$ check nodes at each position. The connections are made as described in [1]. This procedure generates a Tanner graph for the (l,r,L,w) ensemble. The design rate for the (l,r,L,w) ensemble is shown in [1] to be

$$r(l,r,L,w) = \left(1 - \frac{l}{r}\right) - \frac{l}{r} \frac{(w+1) - 2 \sum_{i=0}^w \left(\frac{i}{w}\right)^r}{2L+1}.$$

Two such graphs (generated by the above procedure) are taken and the variable nodes (of each graph) at each position are connected by a random (uniform) permutation of size M via channel nodes. This procedure ensures that all the variable node positions are symmetric and enables us to

write down the density evolution (DE) equations in a simple manner, as described in the following section.

B. Density evolution of the (l,r,L,w) ensemble

Let $\mathbf{a}_i^{(\ell)}$ and $\mathbf{b}_i^{(\ell)}$ denote the average density emitted by the variable node at position i , at iteration ℓ , for codes 1 and 2 respectively. Set $\mathbf{a}_i^{(\ell)} = \mathbf{b}_i^{(\ell)} = \Delta_{+\infty}$ for $i \notin [-L,L]$. The channel densities for codes 1 and 2 are denoted by $\mathbf{a}_{\text{BMS}}^{\text{C}}_1$ and $\mathbf{b}_{\text{BMS}}^{\text{C}}_2$ respectively. All the above densities are L -densities conditioned on the transmission of the all-zero codeword (see Section II). We consider the parallel schedule for each user (as described in [1]) and update the correlation nodes before proceeding to the next iteration. Let us define

$$g(\mathbf{x}_{i-w+1}, \dots, \mathbf{x}_{i+w-1}) \triangleq \left(\frac{1}{w} \sum_{j=0}^{w-1} \left(\frac{1}{w} \sum_{k=0}^{w-1} \mathbf{x}_{i+j-k} \right)^{\boxtimes(r-1)} \right)^{\otimes(l-1)},$$

$$\Gamma(\mathbf{x}_{i-w+1}, \dots, \mathbf{x}_{i+w-1}) \triangleq \left(\frac{1}{w} \sum_{j=0}^{w-1} \left(\frac{1}{w} \sum_{k=0}^{w-1} \mathbf{x}_{i+j-k} \right)^{\boxtimes(r-1)} \right)^{\otimes l}.$$

The DE equations for the joint spatially-coupled system can be written as

$$\begin{aligned} \mathbf{a}_i^{(\ell+1)} &= f_{2 \rightarrow 1} \left(\Gamma(\mathbf{b}_{i-w+1}^{(\ell)}, \dots, \mathbf{b}_{i+w-1}^{(\ell)}), \mathbf{a}_{\text{BAWGNMA}} \right) \otimes \\ &\quad g(\mathbf{a}_{i-w+1}^{(\ell)}, \dots, \mathbf{a}_{i+w-1}^{(\ell)}), \\ \mathbf{b}_i^{(\ell+1)} &= f_{1 \rightarrow 2} \left(\Gamma(\mathbf{a}_{i-w+1}^{(\ell)}, \dots, \mathbf{a}_{i+w-1}^{(\ell)}), \mathbf{a}_{\text{BAWGNMA}} \right) \otimes \\ &\quad g(\mathbf{b}_{i-w+1}^{(\ell)}, \dots, \mathbf{b}_{i+w-1}^{(\ell)}), \end{aligned}$$

for $i \in [-L,L]$. For a further discussion of the DE equations for the (l,r,L,w) spatially-coupled ensembles on BMS channels, see [5]. Using the notation $\underline{\mathbf{a}} \triangleq (\mathbf{a}_{-L}, \dots, \mathbf{a}_L)$, the fixed points of DE are given by $(\mathbf{a}_{\text{BAWGNMA}}, \underline{\mathbf{a}}, \underline{\mathbf{b}})$, which satisfy

$$\begin{aligned} \mathbf{a}_i &= f \left(\Gamma(\mathbf{b}_{i-w+1}, \dots, \mathbf{b}_{i+w-1}), \mathbf{a}_{\text{BAWGNMA}} \right) \otimes \\ &\quad g(\mathbf{a}_{i-w+1}, \dots, \mathbf{a}_{i+w-1}) \\ \mathbf{b}_i &= f \left(\Gamma(\mathbf{a}_{i-w+1}, \dots, \mathbf{a}_{i+w-1}), \mathbf{a}_{\text{BAWGNMA}} \right) \otimes \\ &\quad g(\mathbf{b}_{i-w+1}, \dots, \mathbf{b}_{i+w-1}). \end{aligned} \quad (8)$$

One can use the procedure outlined in [23], known as fixed-entropy DE, to compute both stable and unstable fixed points that satisfy (8).

C. GEXIT curves for the (l,r,L,w) ensemble

Define the GEXIT value of a fixed point $(\mathbf{a}_{\text{BAWGNMA}}, \underline{\mathbf{a}}, \underline{\mathbf{b}})$ by

$$G(\mathbf{a}_{\text{BAWGNMA}}, \underline{\mathbf{a}}, \underline{\mathbf{b}}) \triangleq \frac{1}{2L+1} \sum_{i=-L}^L G(\mathbf{a}_{\text{BAWGNMA}}, \mathbf{a}_i, \mathbf{b}_i).$$

The BP-GEXIT curve $g(\alpha)$, for a fixed A , is the set of points $(\alpha, G(\mathbf{a}_{\text{BAWGNMA}}(\alpha), \underline{\mathbf{a}}, \underline{\mathbf{b}}))$. The resulting curves for the spatially-coupled $(3,6,16,2)$ and $(3,6,32,4)$ ensembles are shown in Fig. 6 for symmetric channel conditions. These curves are very similar to the single user case and demonstrate the phenomenon of threshold saturation at the joint decoder, for symmetric channel conditions. For channel parameters not on the symmetric line, these plots imply threshold saturation towards the MAP boundary.

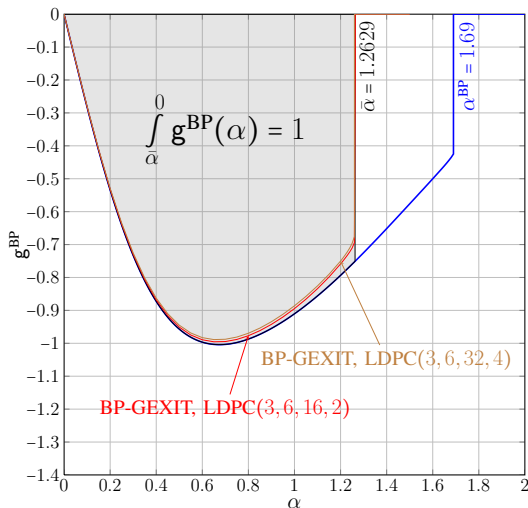


Fig. 6. BP-GEXIT curves of the $(3, 6, L, w)$ spatially-coupled LDPC and $(3, 6)$ regular LDPC ensembles for transmission over a 2-user binary-input Gaussian MAC, with $A = 1$. Also shown is the upper bound on the MAP threshold for the $(3, 6)$ regular LDPC ensemble, computed using the area theorem.

IV. RESULTS AND CONCLUDING REMARKS

It was shown in [1], that for transmission over a BEC, the BP threshold of spatially-coupled ensembles is essentially equal to the MAP threshold of the underlying ensemble. This was observed numerically for general BMS channels in [5], [3]. It was observed numerically for multi-user scenarios in [7], [8]. The notion of universality with respect to channel parameters is important for multi-terminal problems and has been discussed in [7], [14], [25].

In this paper, we study the 2-user binary-input Gaussian MAC and observe that spatial coupling boosts the BP-ACPR of the joint decoder to the MAP-ACPR of the underlying ensemble. The BP-ACPR for the scenarios considered in this paper are shown in Fig. 7 and these results confirm the preliminary results reported in [7]. This figure shows that spatially-coupled ensembles are near universal for this problem. Based on the observation that regular LDPC codes with large left degrees behave like random codes and the fact that random codes are universal under MAP decoding, we also conjecture that increasing the left degree (keeping the rate constant) will push the MAP boundary towards the boundary of the MAC-ACPR. An analytic proof of threshold saturation remains an open problem. Such a proof would essentially show that it is possible to achieve universality for the 2-user binary-input Gaussian MAC under iterative decoding.

This work can be extended in a variety of ways. For example, it is straightforward to dispense with AWGN and compute the ACPRs of any suitably parameterized 2-user binary-input MAC. One can also generalize these results to m -user MACs, larger input alphabets, and multiple-input multiple-output (MIMO) systems. In these cases, the increase in computational complexity makes discretized DE infeasible and Monte Carlo methods must be used to evaluate the DE and GEXIT functions. We conjecture that threshold saturation will continue to occur for all these extensions

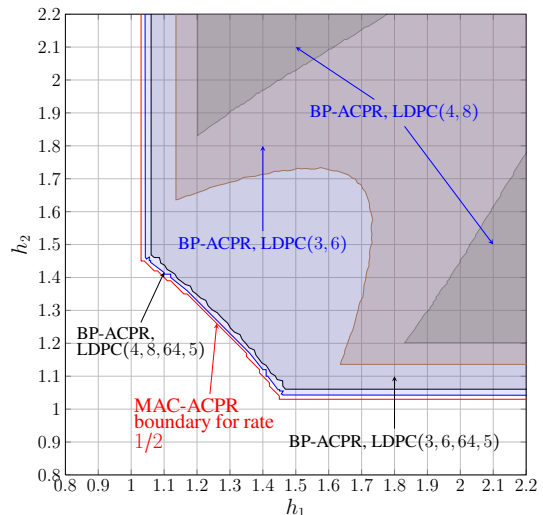


Fig. 7. BP-ACPR of the $(3, 6, 64, 5)$ and $(4, 8, 64, 5)$ spatially-coupled LDPC ensembles for the 2-user binary-input Gaussian MAC. Also shown are the BP-ACPRs for the $(3, 6)$ and $(4, 8)$ regular LDPC ensembles. The BP-ACPR of the $(4, 8, 64, 5)$ spatially-coupled LDPC ensemble is very close to the MAC-ACPR, demonstrating the near-universal performance of spatially-coupled codes.

and that spatially-coupled codes will achieve near-universal performance.

REFERENCES

- [1] S. Kudekar, T. Richardson, and R. Urbanke, "Threshold saturation via spatial coupling: Why convolutional LDPC ensembles perform so well over the BEC," *IEEE Trans. Inform. Theory*, vol. 57, no. 2, pp. 803–834, 2011.
- [2] J. Felstrom and K. S. Zigangirov, "Time-varying periodic convolutional codes with low-density parity-check matrix," *IEEE Trans. Inform. Theory*, vol. 45, no. 6, pp. 2181–2191, 1999.
- [3] M. Lentmaier, A. Sridharan, K. Zigangirov, and D. J. Costello, "Terminated LDPC convolutional codes with thresholds close to capacity," in *Proc. IEEE Int. Symp. Inform. Theory*, Adelaide, Australia, 2005, pp. 1372–1376.
- [4] M. Lentmaier and G. Fettweis, "On the thresholds of generalized LDPC convolutional codes based on protographs," in *Proc. IEEE Int. Symp. Inform. Theory*, Austin, TX, 2010, pp. 709–713.
- [5] S. Kudekar, C. Méasson, T. Richardson, and R. Urbanke, "Threshold saturation on BMS channels via spatial coupling," in *Proc. Int. Symp. on Turbo Codes & Iterative Inform. Proc.*, Sept. 2010, pp. 309–313.
- [6] S. Kudekar and K. Kasai, "Threshold saturation on channels with memory via spatial coupling," in *Proc. IEEE Int. Symp. Inform. Theory*, St. Petersburg, Russia, July 2011, pp. 2562–2566.
- [7] A. Yedla, H. Pfister, and K. Narayanan, "Universality for the noisy Slepian-Wolf problem via spatial coupling," in *Proc. IEEE Int. Symp. Inform. Theory*, St. Petersburg, Russia, July 2011, pp. 2567–2571.
- [8] S. Kudekar and K. Kasai, "Spatially coupled codes over the multiple access channel," in *Proc. IEEE Int. Symp. Inform. Theory*, St. Petersburg, Russia, July 2011, pp. 2816–2820.
- [9] V. Rathi, R. Urbanke, M. Andersson, and M. Skoglund, "Rate-equivocation optimally spatially coupled LDPC codes for the BEC wiretap channel," in *Proc. IEEE Int. Symp. Inform. Theory*, St. Petersburg, Russia, July 2011, pp. 2393–2397.
- [10] S. Hassani, N. Macris, and R. Urbanke, "Coupled graphical models and their thresholds," in *Proc. IEEE Inform. Theory Workshop*, Dublin, Ireland, 2010, pp. 1–5.
- [11] S. Kudekar and H. Pfister, "The effect of spatial coupling on compressive sensing," in *Proc. Annual Allerton Conf. on Commun., Control, and Comp.*, Monticello, IL, Oct. 2010, pp. 347–353.
- [12] D. Tse and P. Viswanath, *Fundamentals of wireless communication*. Cambridge, 2005.
- [13] S. Tavildar and P. Viswanath, "Approximately universal codes over slow-fading channels," *IEEE Trans. Inform. Theory*, vol. 52, no. 7, pp. 3233–3258, 2006.

- [14] A. Yedla, H. D. Pfister, and K. R. Narayanan, "Can iterative decoding for erasure correlated sources be universal?" in *Proc. 47th Annual Allerton Conf. on Commun., Control, and Comp.*, Monticello, IL, Sept. 2009.
- [15] R. Palanki, A. Khandekar, and R. J. McEliece, "Graph-based codes for synchronous multiple access channels," in *Proc. Annual Allerton Conf. on Commun., Control, and Comp.*, vol. 39, no. 2, 2001, pp. 1263–1271.
- [16] B. Rimoldi and R. Urbanke, "A rate-splitting approach to the Gaussian multiple-access channel," *IEEE Trans. Inform. Theory*, vol. 42, no. 2, pp. 364–375, 1996.
- [17] A. Amraoui, S. Dusad, and R. Urbanke, "Achieving general points in the 2-user Gaussian MAC without time-sharing or rate-splitting by means of iterative coding," in *Proc. IEEE Int. Symp. Inform. Theory*, 2002, p. 334.
- [18] A. Roumy and D. Declercq, "Characterization and optimization of LDPC codes for the 2-user Gaussian multiple access channel," *EURASIP J. on Wireless Commun. and Networking*, vol. Article ID, no. 74890, 2007.
- [19] R. Liu, P. Spasojevic, and E. Soljanin, "Reliable channel regions for good binary codes transmitted over parallel channels," *IEEE Trans. Inform. Theory*, vol. 52, no. 4, pp. 1405–1424, 2006.
- [20] T. J. Richardson and R. L. Urbanke, *Modern Coding Theory*. Cambridge, 2008.
- [21] S. Chung, G. D. Forney, Jr., T. J. Richardson, and R. L. Urbanke, "On the design of low-density parity-check codes within 0.0045 dB of the Shannon limit," *IEEE Commun. Letters*, vol. 5, no. 2, pp. 58–60, Feb. 2001.
- [22] C. Méasson, "Conservation laws for coding," Ph.D. dissertation, Swiss Federal Institute of Technology, Lausanne, 2006.
- [23] C. Méasson, A. Montanari, T. Richardson, and R. Urbanke, "The generalized area theorem and some of its consequences," *IEEE Trans. Inform. Theory*, vol. 55, no. 11, pp. 4793–4821, Nov. 2009.
- [24] A. Sridharan, M. Lentmaier, D. J. Costello, and K. S. Zigangirov, "Convergence analysis of a class of LDPC convolutional codes for the erasure channel," in *Proc. Annual Allerton Conf. on Commun., Control, and Comp.*, Monticello, IL, 2004, pp. 953–962.
- [25] A. Yedla, H. D. Pfister, and K. R. Narayanan, "LDPC code design for transmission of correlated sources across noisy channels without CSIT," in *Proc. Int. Symp. on Turbo Codes & Iterative Inform. Proc.*, Brest, France, Sept. 2010, pp. 474–478.